Journal of Manufacturing Processes 115 (2024) 40–55

Contents lists available at ScienceDirect

Journal of Manufacturing Processes

journal homepage: www.elsevier.com/locate/manpro

Convection and joint characteristics in aluminum alloy melting zone during resistance spot welding of dissimilar Fe-Al material in external magnetic field

Yuta Funabiki [a], Muneyoshi Iyota [a,*], Takahisa Shobu [b], Tomoki Matsuda [c], Hirokatsu Yumoto [d,e], Takahisa Koyama [d,e], Hiroshi Yamazaki [d,e], Yasunori Senba [d,e], Haruhiko Ohashi [d,e], Ichiro Inoue [e], Gota Yamaguchi [e], Yujiro Hayashi [e], Makina Yabashi [e], Tomokazu Sano [c]

[a] Department of Mechanical Engineering, Faculty of Engineering, Osaka Institute of Technology, 5-16-1 Omiya Asahi-ku, Osaka 535-8585, Japan
[b] Materials Sciences Research Center, Japan Atomic Energy Agency, 2-4 Shirakata, Tokai-mura, Ibaraki 319-1195, Japan
[c] Division of Materials and Manufacturing Science, Graduate School of Engineering, Osaka University, 2-1 Yamadaoka, Suita, Osaka 565-0871, Japan
[d] Japan Synchrotron Radiation Research Institute, 1-1-1 Kouto, Sayo-cho, Sayo-gun, Hyogo 679-5198, Japan
[e] RIKEN SPring-8 Center, 1-1-1 Kouto, Sayo-cho, Sayo-gun, Hyogo 679-5148, Japan

ARTICLE INFO

Keywords:
Resistance spot welding
Dissimilar materials joining
Convection
External magnetic field
Synchrotron radiation
Intermetallic compound
Cross tension strength

ABSTRACT

In resistance spot welding (RSW) of Fe and Al alloy, an intermetallic compound (IMC) is formed at the joining interface, and it is known that the strength of the joint decreases as the IMC becomes thicker. One of the factors that determines the thickness of the IMC is the temperature field during welding, which is considered to vary greatly depending on convection within the Al alloy melting zone. Therefore, changes in convection are considered to possibly affect the state of IMC formation, but there have been few detailed studies of this phenomenon. In this study, convection in the Al alloy melting zone of an Fe-Al alloy RSW was varied and the effect on the joint characteristics was investigated. For this study, to focus on the electromagnetic force generated in the Al alloy melting zone, convection in the Al alloy melting zone was changed by applying a magnetic field using neodymium magnets. In-situ evaluation of the convection using synchrotron radiation and cross-sectional images of the joint revealed that the presence of a magnetic field during welding causes a non-axisymmetric change in convection in the Al alloy melting zone, which deflects this zone. The magnetic field increases the driving force for convection and homogenizes the temperature field at the joining interface, leading to the formation of a thin uniform IMC near the joint center. Furthermore, from a cross tension test and observation of the fracture surface of the joint after the test, it was clarified that the cross tension strength of the joint welded under a magnetic field was improved by the propagation of cracks into the Al alloy melting zone during the test.

1. Introduction

In recent years, the automotive industry has been seeking to improve the fuel efficiency of vehicles from the viewpoint of reducing environmental problems caused by vehicle emissions, and has been promoting weight reduction of vehicle bodies. One method to reduce the weight of car bodies is to combine steel (Fe) and aluminum (Al) alloy to create a multi-material car body. To realize this, a dissimilar metal joining technique for Fe and Al alloy is required. There are various types of dissimilar metal joining techniques, such as resistance spot welding (RSW) [1–10], friction stir spot welding [11,12], and laser welding [13,14], but RSW is mainly used for fabricating car bodies, and because this joining technique has many advantages, the joining of Fe and Al alloy using RSW has attracted much attention.

However, it is known that in RSW of Fe and Al alloy, an intermetallic compound (IMC) is formed at the joining interface, and if this IMC is thick, the strength of the joint is greatly reduced [1–3]. Therefore, it is necessary to form a thin and uniform IMC to ensure sufficient joint strength. Because IMC formation depends on temperature [4], controlling the temperature field at the joining interface during welding is considered to be an effective method for forming a thin IMC. In the past, many studies have focused on the temperature field at the joining

* Corresponding author.
E-mail address: muneyoshi.iyota@oit.ac.jp (M. Iyota).

https://doi.org/10.1016/j.jmapro.2024.01.049
Received 5 October 2023; Received in revised form 2 January 2024; Accepted 16 January 2024

Table 1
Chemical composition of each material.

	C	Si	Mn	P	S	Fe	Cu	Mg	Cr	Zn	Ti	Al
GA590	0.12	0.29	1.41	0.009	0.305	Bal.	–	–	–	–	–	–
A6061-T6	–	0.7	0.12	–	–	0.4	0.29	1.1	0.17	0.03	0.03	Bal.

Table 2
Welding conditions.

Current, I (kA)	Current time, t (ms)	Electrode force, F (kN)	Hold time, t_h (ms)	External magnetic field
14.0	200	5.0	100	Without With

interface during welding, such as studies focusing on electrode geometry [5,6] and the use of an intermediate layer [7,8].

However, because the Al alloy becomes molten during welding, convection currents may be generated in the Al alloy melting zone. Because this zone is always in contact with the joining interface, the temperature field at the joining interface may change due to heat transport by convection in the Al alloy melting zone. Convection of molten metal has been widely studied in arc and laser welding, and direct observations have revealed that it affects the temperature field during welding [15–17]. Some studies on convection in molten metal during RSW have also been conducted [18], not only for welding Fe to Fe, but also for joining dissimilar metals such as Fe and Al alloy. From previous studies, experimental and numerical simulations have revealed the existence of convection in the Al alloy melting zone of RSW of Fe and Al alloy [19,20]. Based on these findings, changes in convection within the Al alloy melting zone during welding are considered likely to affect the formation of the IMC, which depends on the temperature field at the joining interface. In fact, it has been reported that in Fe-Al dissimilar material RSW using an external magnetic field, IMC is formed thinly overall due to the circular motion of the melting metal caused by the electromagnetic force [9]. However, even with a magnetic field, the thickness of the IMC near the center remained thicker than that at the edge. Considering ensuring sufficient joint strength, it is assumed that the IMC should be thin and uniformly formed not only at the edge but also near the center. In addition, few studies have examined the effect of melting metal flow, or convection, on the temperature field at the

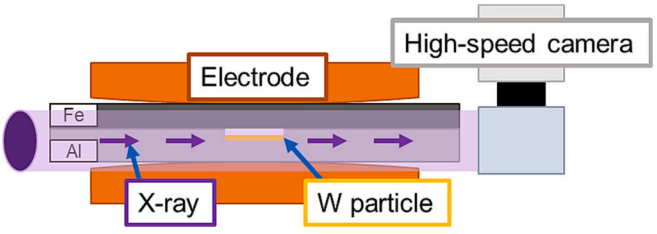

Fig. 2. X-ray irradiation method.

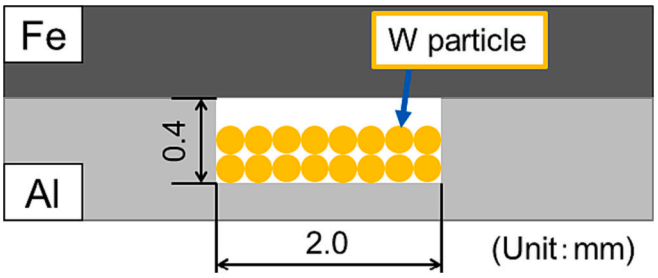

Fig. 3. Arrangement of W particles.

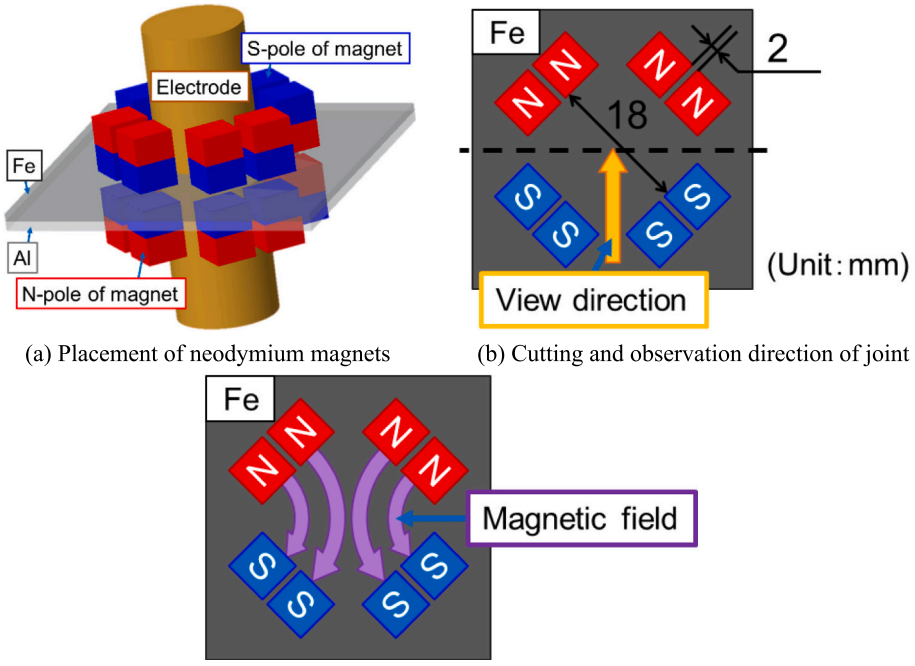

(a) Placement of neodymium magnets (b) Cutting and observation direction of joint

(c) Magnetic field distribution by neodymium magnets

Fig. 1. Method for applying magnetic field. (a) Placement of neodymium magnets. (b) Cutting and observation direction of joint. (c) Magnetic field distribution by neodymium magnets.

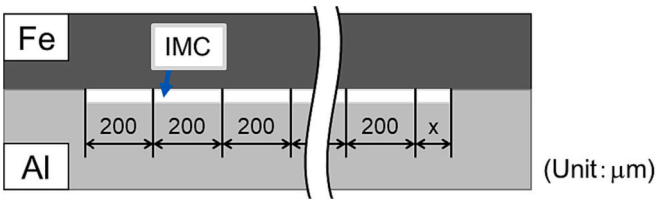

Fig. 4. Obtaining IMC thickness distribution.

joining interface, and the relationship between convection, IMC, and joint strength has not been clarified.

In this study, the effect of convection in the Al alloy melting zone on the joint characteristics in Fe-Al dissimilar material RSW was investigated by welding with a new method of applying a magnetic field that allowed the formation of a thinner and more uniform IMC near the center than was previously possible. The main feature of this experiment is that a real-scale specimen and an RSW apparatus used in actual production were used to observe the convection of the joint to which a magnetic field was applied. In this experiment, X-ray transmission images were taken of the joint during welding using synchrotron radiation, and the convection in the Al alloy melting zone of the joint under a magnetic field was observed, allowing the convection velocity to be calculated. Next, cross-sectional observations of the joint and temperature measurements of the joining interface were conducted, and the relationship between the change in convection and the shape of the Al alloy melting zone and the thickness of the IMC due to the applied magnetic field was explored. Furthermore, to understand the change in cross tension strength (CTS) and crack propagation behavior due to changes in convection in the Al alloy melting zone, cross tension testing was conducted on the joint welded in the presence of a magnetic field, and the fracture surface of the joint was observed after the test.

2. Experimental conditions

2.1. Test material and welding procedure

The test specimens were 590-MPa class alloyed hot-dip galvanized steel sheets (Fe) with a thickness of 1.2 mm and A6061 alloy sheets (Al alloy) with a thickness of 1.6 mm. The chemical composition of each material is shown in Table 1. Specimen dimensions were 50 mm × 50 mm. A C-type gun RSW welding machine with a DC inverter power supply was used. During welding, Fe was placed on the positive electrode and Al alloy on the negative electrode. The power supply

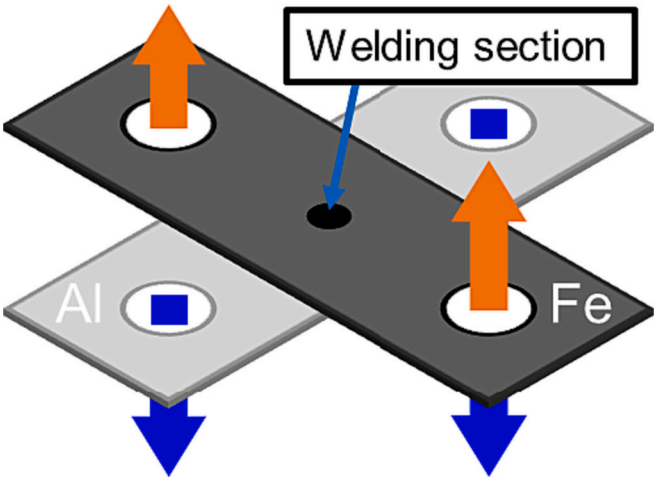

Fig. 6. Load direction in cross tension test.

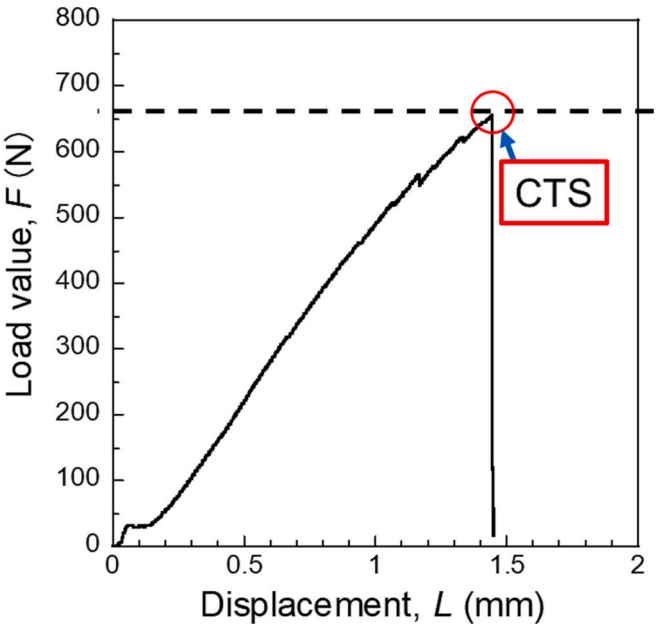

Fig. 7. Load-displacement curve.

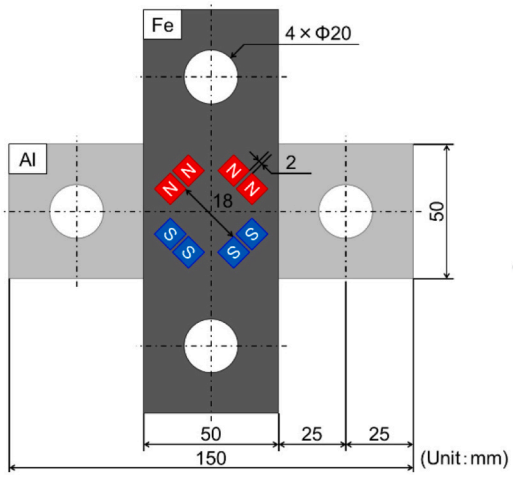

(a) Dimension of specimen

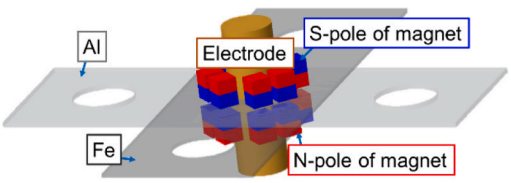

(b) Placement of neodymium magnets

Fig. 5. Applying magnetic field to cross tension specimen. (a) Dimension of specimen. (b) Placement of neodymium magnets.

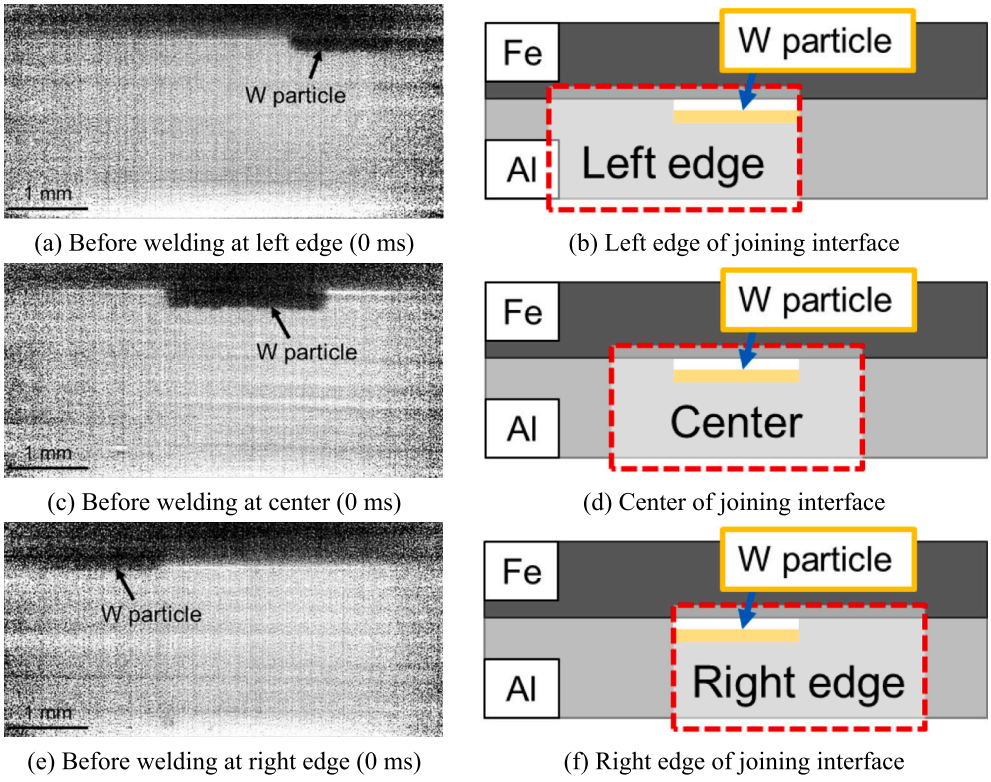

(a) Before welding at left edge (0 ms) (b) Left edge of joining interface

(c) Before welding at center (0 ms) (d) Center of joining interface

(e) Before welding at right edge (0 ms) (f) Right edge of joining interface

Fig. 8. Positions for observing convection. (a) Before welding at left edge (0 ms). (b) Left edge of joining interface. (c) Before welding at center (0 ms). (d) Center of joining interface. (e) Before welding at right edge (0 ms). (f) Right edge of joining interface.

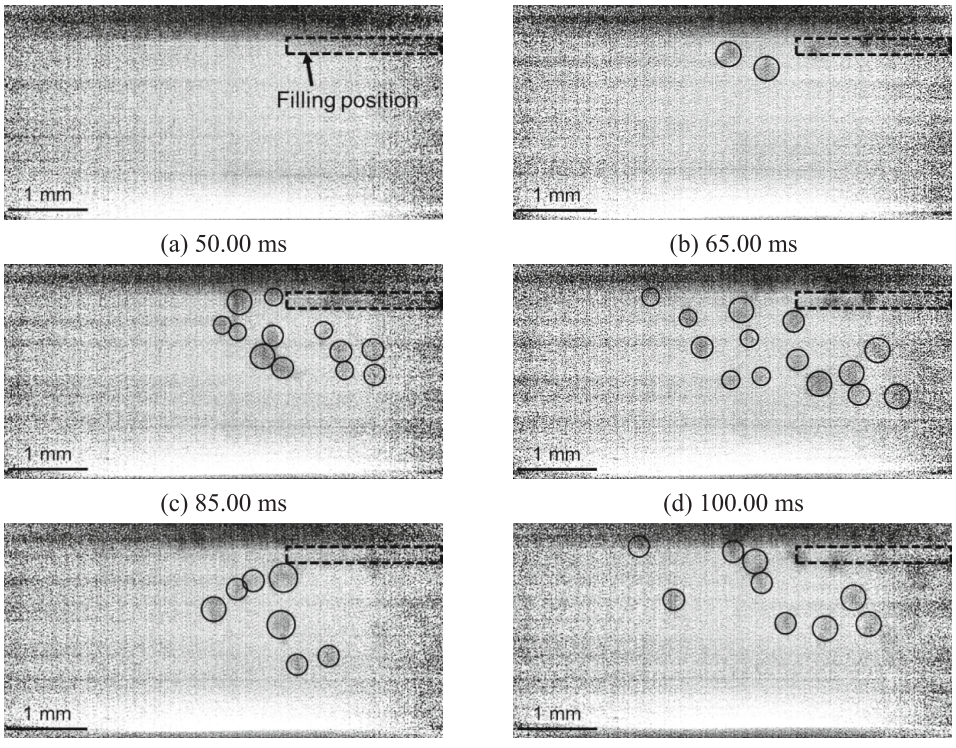

(a) 50.00 ms (b) 65.00 ms

(c) 85.00 ms (d) 100.00 ms

(e) 150.00 ms (f) 200.00 ms

Fig. 9. Behavior of W particles during welding at left edge. (a) 50.00 ms. (b) 65.00 ms. (c) 85.00 ms. (d) 100.00 ms. (e) 150.00 ms. (f) 200.00 ms.

frequency was 60 Hz. The welding conditions are shown in Table 2. The electrodes were R-shaped and made of alumina dispersion-strengthened copper (Al_2O_3Cu) with a diameter of 16 mm and a tip curvature of 100 mm.

Regarding the new method of applying a magnetic field used in this experiment, as described in the previous chapter, welding using the

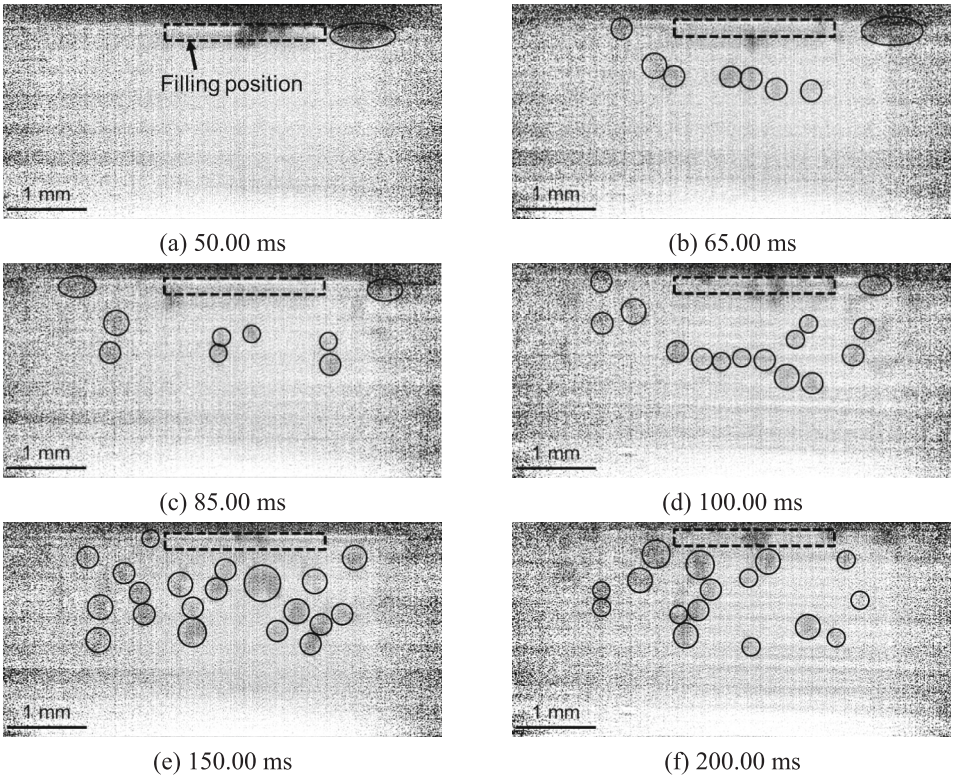

Fig. 10. Behavior of W particles during welding at center. (a) 50.00 ms. (b) 65.00 ms. (c) 85.00 ms. (d) 100.00 ms. (e) 150.00 ms. (f) 200.00 ms.

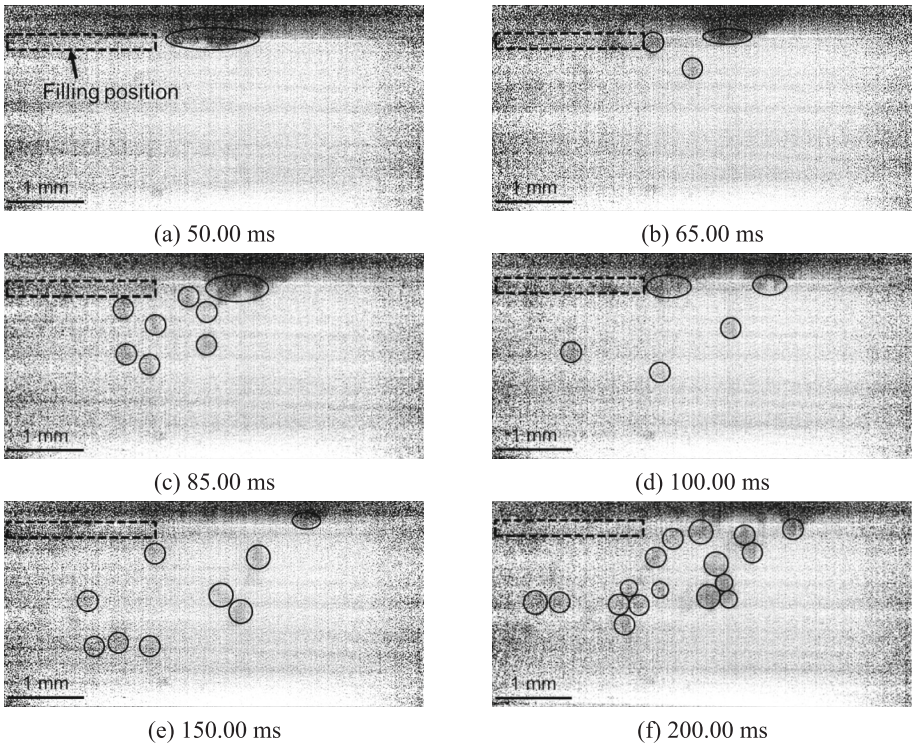

Fig. 11. Behavior of W particles during welding at right edge. (a) 50.00 ms. (b) 65.00 ms. (c) 85.00 ms. (d) 100.00 ms. (e) 150.00 ms. (f) 200.00 ms.

conventional method results in a thicker IMC near the center compared to the edge [9]. This is thought to be due to the higher temperature in the center of the joining interface compared to the edge. Therefore, in this experiment, with the aim of stirring the melting metal at the center and lowering the temperature at the center of the joining interface by generating high speed convection near the center of the joining interface in the Al alloy melting zone, welding was performed using a new method of applying a magnetic field by placing neodymium magnets as shown in Fig. 1. The magnets have a length of 6.5 mm, a width of 6.5 mm, and a height of 9.0 mm (in the direction of magnetization). The surface

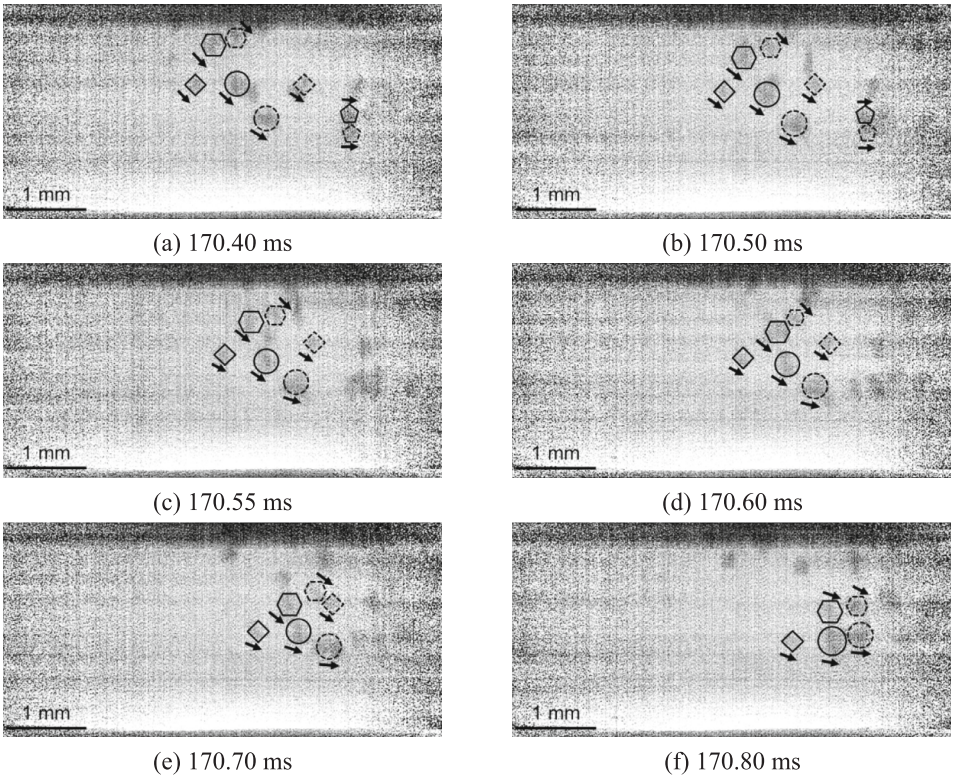

Fig. 12. Behavior of W particles in late stage of welding at left edge. (a) 170.40 ms. (b) 170.50 ms. (c) 170.55 ms. (d) 170.60 ms. (e) 170.70 ms. (f) 170.80 ms.

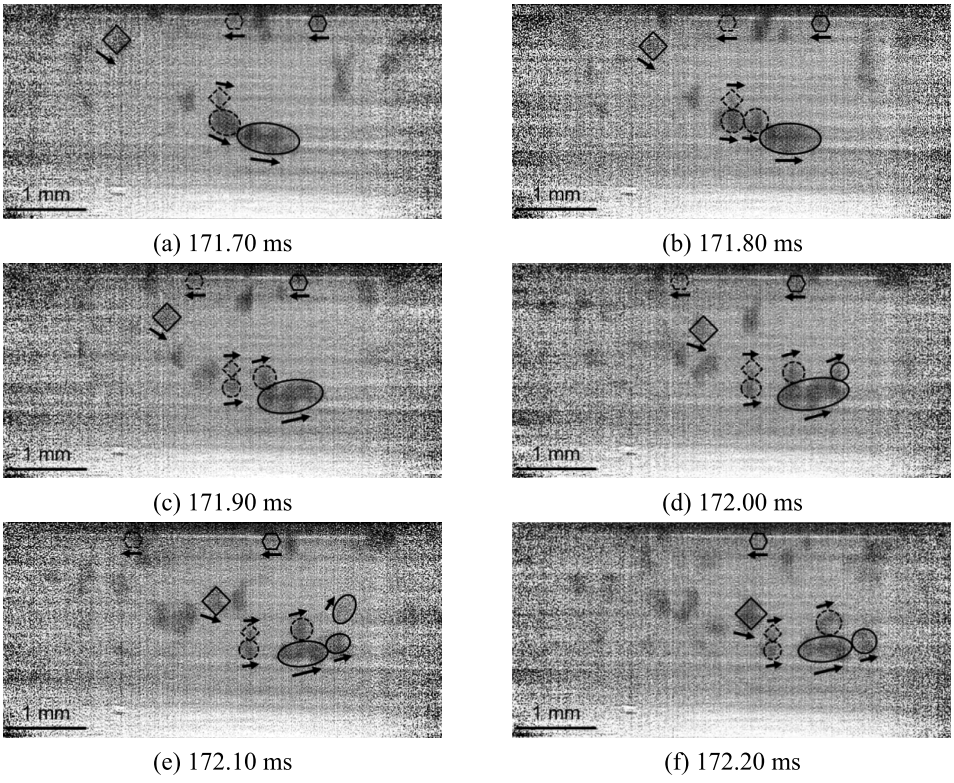

Fig. 13. Behavior of W particles in late stage of welding at center. (a) 171.70 ms. (b) 171.80 ms. (c) 171.90 ms. (d) 172.00 ms. (e) 172.10 ms. (f) 172.20 ms.

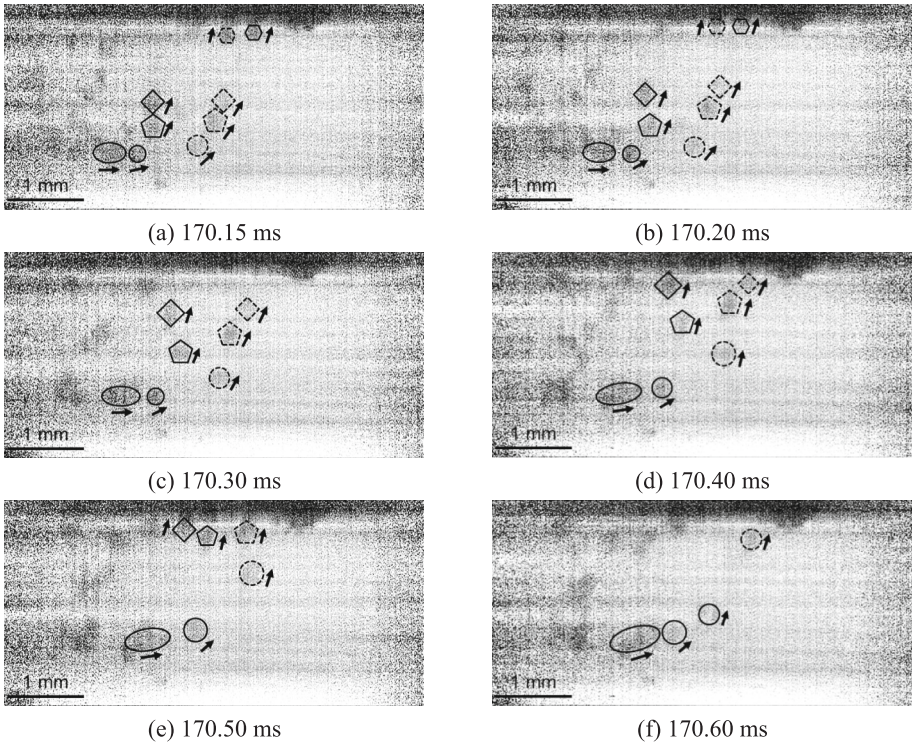

Fig. 14. Behavior of W particles in late stage of welding at right edge. (a) 170.15 ms. (b) 170.20 ms. (c) 170.30 ms. (d) 170.40 ms. (e) 170.50 ms. (f) 170.60 ms.

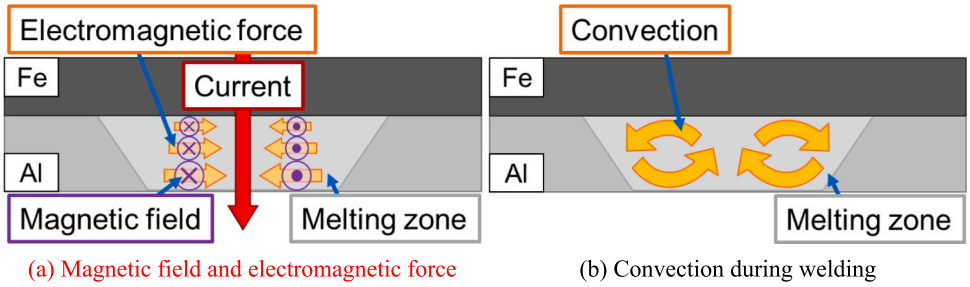

Fig. 15. Process for generation of convection in joint without magnetic field. (a) Current and magnetic field during welding. (b) Convection during welding.

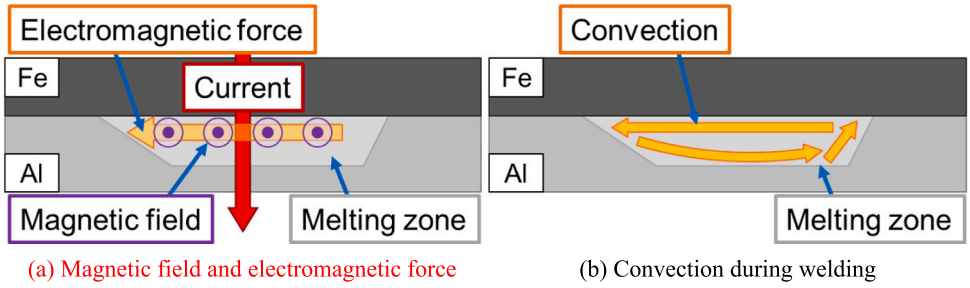

Fig. 16. Process for generation of convection in joint with magnetic field. (a) Current and magnetic field during welding. (b) Convection during welding.

magnetic flux density is 578 mT.

2.2. Observing convection using tracer particles

In-situ evaluation of convection in the Al alloy melting zone using synchrotron radiation was performed at the RIKEN Contract Beamline BL05XU at SPring-8, based on experiments conducted in previous studies [19]. Light with an energy bandwidth of approximately 0.93 % was used, which was formed by shaping 100-keV light, the primary light of the 5.26-keV fundamental wave from the undulator, using a multilayer mirror. These X-ray were shaped to a width of 4.0 mm by a slit and expanded to a height of 3.0 mm by a magnifying optical mirror. The X-ray irradiated the specimen being welded, and the convection in the Al alloy melting zone was observed by acquiring X-ray transmission images. The X-ray propagation direction was along the specimen plane as shown in Fig. 2 in order to determine the change in convection in the cross section of the Al alloy melting zone during welding. The direction of observation of the joint is indicated by the yellow arrow in Fig. 1(b). A

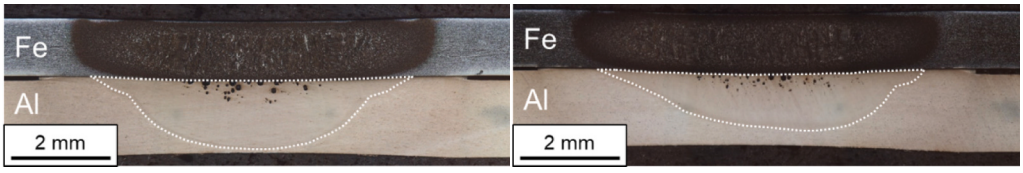

(a) Without magnetic field (b) With magnetic field

Fig. 17. Cross-sectional photographs of joints without and with magnetic field. (a) Without magnetic field. (b) With magnetic field.

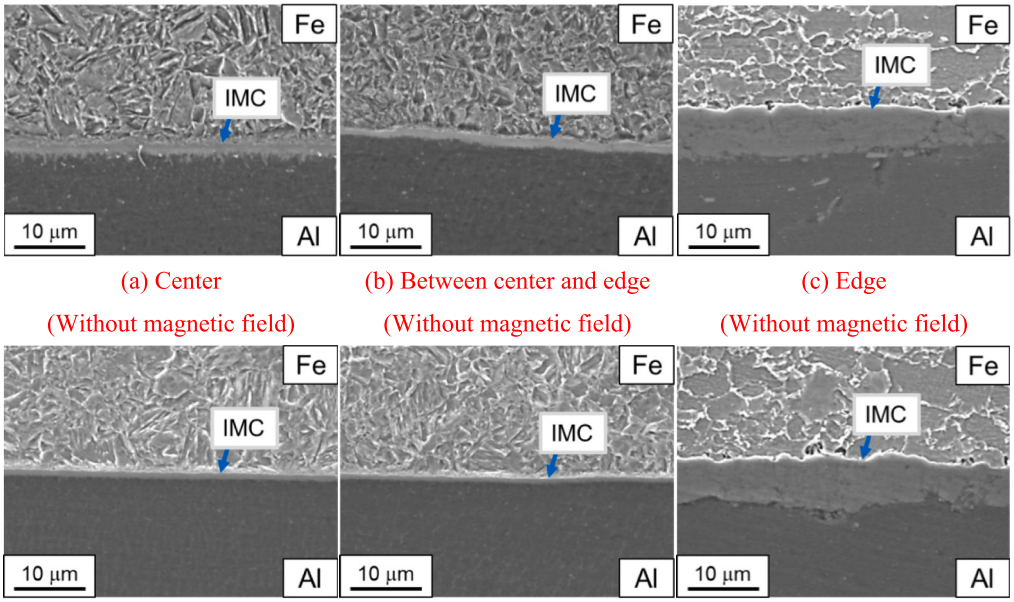

Fig. 18. IMC from center to edge of joints without and with magnetic field. (a) Center (Without magnetic field). (b) Between center and edge (Without magnetic field). (c) Edge (Without magnetic field). (d) Center (With magnetic field). (e) Between (With magnetic field). (f) Edge (With magnetic field).

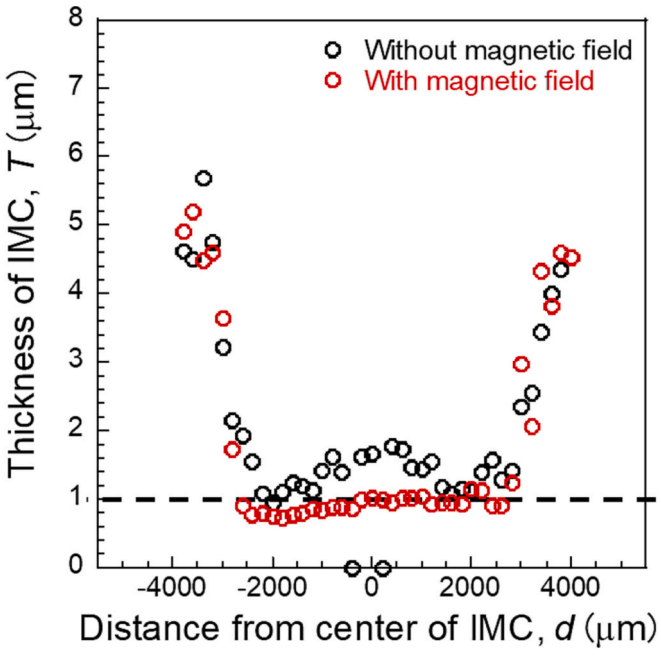

Fig. 19. IMC thickness distribution for joints without and with magnetic field.

high-speed camera was used to acquire X-ray transmission images at an acquisition frequency of 20,000 Hz.

In this experiment, as shown in Fig. 3, a groove with a diameter of 2.0 mm and a depth of 0.4 mm was machined in the center of the surface of the Al alloy joining interface, and tungsten (W) particles with a diameter of 150 μm were filled into this groove as tracer particles during welding.

2.3. Cross-sectional observations and IMC thickness distribution

For the cross-sectional observation method, the welded joint was first cut along the dashed line shown in Fig. 1(b) and embedded in resin using a mold forming machine. The specimen was then polished with water-resistant abrasive paper. Finally, the specimen was buffed to a mirror finish and etched for 30 s using a 3 % nital solution. Cross-sectional observations were performed using an Olympus DX510 digital microscope. The observation direction was as indicated by the yellow arrow in Fig. 1(b).

IMC observations were performed using a scanning electron microscope (SEM; JEOL JCM-7000 tabletop scanning electron microscope). For the IMC thickness distribution acquiring method, as shown in Fig. 4, the area where an IMC was formed was photographed at 200-μm intervals from the left end to the right end. The IMC thickness distribution was then obtained by measuring the IMC thickness in five points randomly chosen in all photographs and then averaging the acquired values.

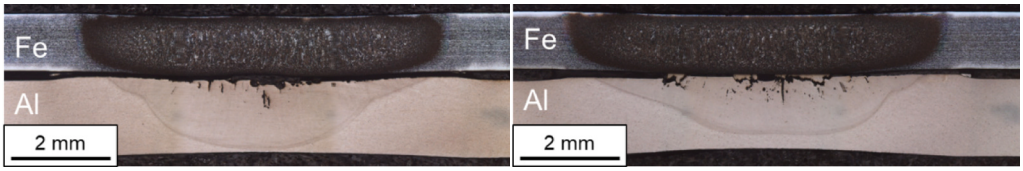

(a) Without magnetic field (b) With magnetic field

Fig. 20. Cross-sectional photographs of joints after joints after cross tension tests. (a) Without magnetic field. (b) With magnetic field.

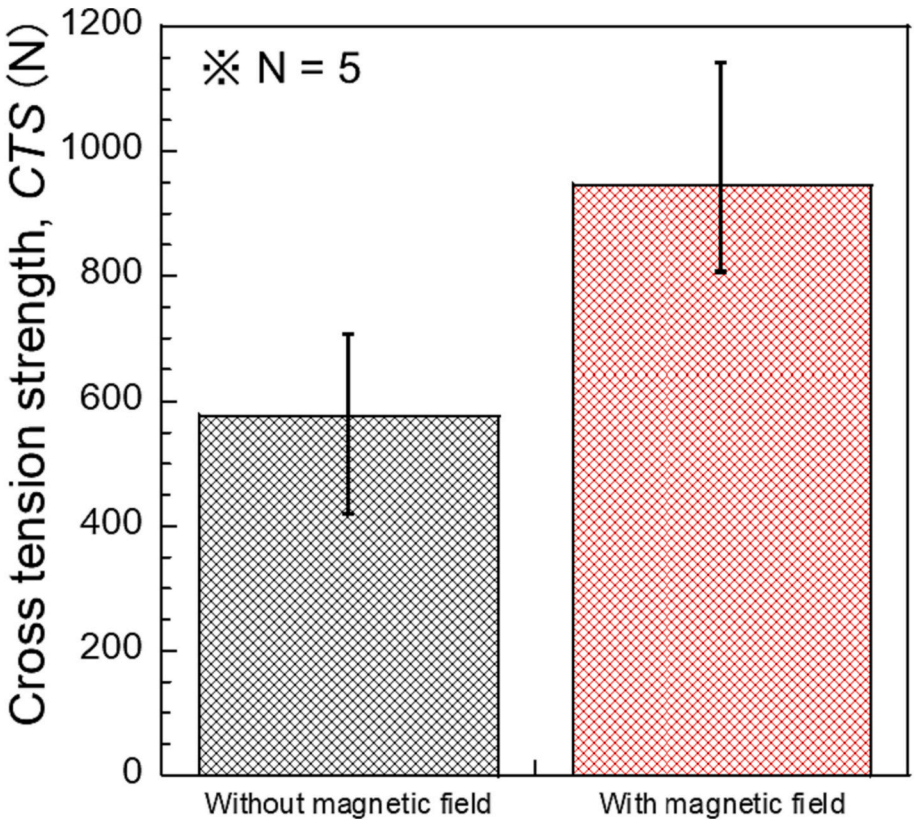

Fig. 21. Cross tension strength of joints without and with magnetic field.

2.4. Cross tension test and joint fracture surface observations

A cross tension test was conducted using a cross tension welding specimen with the dimensions shown in Fig. 5(a). The arrangement of the neodymium magnets on the specimen is shown in Fig. 5(b). The test conditions were in accordance with JIS Z 3137, with a tensile speed of 5.0 mm/min and the loading direction shown in Fig. 6. As shown in Fig. 7, the joint CTS in the peeling direction was evaluated as the value with the highest load in the load-displacement curve obtained in the cross tension test.

SEM and energy-dispersive X-ray spectroscopy (EDS) were used to observe the fracture surface and conduct an elemental analysis of the cross tension tested joint. Fracture surface observations and elemental analyses were performed on both the Fe side and the Al alloy side.

3. Results

3.1. In-situ evaluation of convection using synchrotron radiation

Fig. 8 shows the observation positions in the X-ray transmission image of the specimen before welding and the convection in the in-situ evaluation. The observation positions are the center, left edge, and right edge, and the field of view is fixed at the point where W particles filled before welding can be clearly observed. The images are cropped to make the behavior of W particles in the Al alloy melting zone during welding clearly visible. The current time during X-ray transmission image acquisition was calculated from the number of images taken and the imaging frequency, with the time just before the W particles moved out of the filling position set to 0 ms.

Figs. 9, 10, and 11 show the behavior of W particles from the start to the end of energization at the left edge, center, and right edge of the joint under a magnetic field, respectively. These figures show that the W particles, as indicated by the black circles, moved in the radial direction near the joining interface from the filling position from 50.00 ms to 65.00 ms and then diffused in the thickness direction along the solid-liquid interface from 85.00 ms to 200.00 ms at each observation position. This suggests that the W particles were moved by convection in the Al alloy melting zone. However, the movement of the W particles was too rapid to capture the direction of the convection current.

Figs. 12, 13, and 14 show the behavior of W particles during the late stage of energization at the left edge, center, and right edge of the joint under a magnetic field, respectively. Fig. 12 shows that W particles moved from the left edge of the Al alloy melting zone toward the bottom along the solid-liquid interface, as indicated by each frame and black

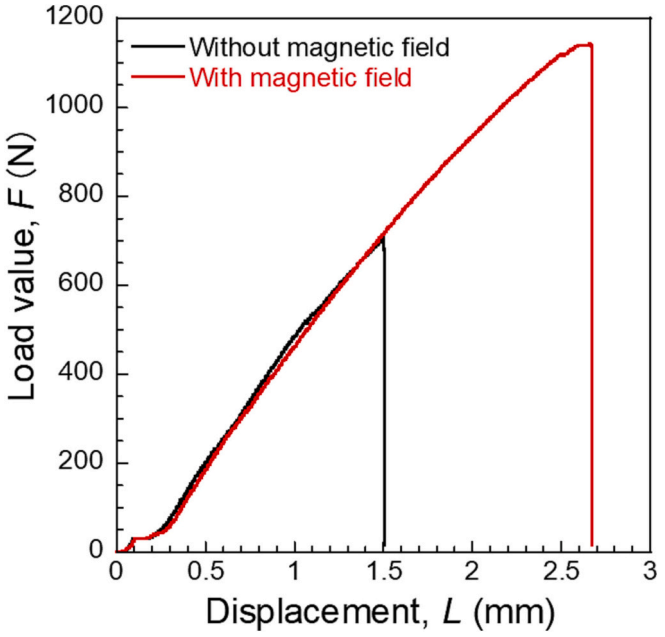

Fig. 22. Load-displacement curve of joints without and with magnetic field.

arrows. In addition, Fig. 13 shows that, at the center, W particles moved from the right side toward the left side along the joining interface, and from the left side toward the right side along the solid-liquid interface of the Al alloy melting zone. In addition, Fig. 14 shows that W particles moved from the left side along the solid-liquid interface of the Al alloy melting zone toward the right edge.

As the reason for these results, a magnetic field is generated in the Al alloy melting zone by the current during welding in the joint without a magnetic field, as shown in Fig. 15(a). Therefore, previous studies have reported that an electromagnetic force perpendicular to the magnetic field was generated during energization, resulting in convection in the radial and thickness directions in the Al alloy melting zone, as shown in Fig. 15(b) [19,20]. In contrast, in this experiment, the N and S poles of the neodymium magnets were arranged non-axisymmetrically and welding was performed as shown in Fig. 1. Then, a unidirectional magnetic field passing through the Al alloy melting zone was applied, as shown Fig. 16(a). Therefore, an electromagnetic force perpendicular to the magnetic field was generated during energization, likely driving convection in a non-axisymmetric manner in the Al alloy melting zone, as shown Fig. 16(b). It was inferred that W particles moved in a non-axisymmetric manner in the Al alloy melting zone of the joint welded in the presence of a magnetic field. These results suggest that the presence of the magnetic field changed the convection in the Al alloy melting zone in a non-axisymmetric manner.

3.2. Al alloy melting zone shape and IMC thickness

Cross-sectional photographs of the joints welded without and with a magnetic field are shown in Fig. 17. The white dotted lines indicate the Al alloy melting zone. It can be seen that the Al alloy melting area in the joint with a magnetic field does not expand in the thickness direction and is deflected to the right side compared to the joint without a magnetic field. Based on the results of the in-situ evaluation described in the previous section, non-axisymmetric convection is considered to have occurred in the Al alloy melting zone under a magnetic field. This is thought to have deflected the melting zone rather than expanding it in the sheet thickness direction.

Fig. 18 shows the IMC from the center to the edge for joints welded without and with a magnetic field, and Fig. 19 shows the IMC thickness distribution at each joint. From these figures, the IMC is seen to be thicker at the edge of the joint in both joints. It has been reported that in the joining of galvanized steel sheet and Al alloy, an Al-zinc (Zn) eutectic melt is generated at the joining interface due to the eutectic reaction between Zn and Al in galvanized plating, and this eutectic melt is discharged to the edge by pressurization and subsequently combines with the Fe-Al compound to form a mixed phase [1,21]. This suggests that the eutectic melt discharged at the edge is replaced by the IMC so that the IMC at the edge is thicker. In contrast, examination of the area near the center shows that an IMC with a thickness exceeding 1 μm was formed in the joint without a magnetic field, while an IMC with a thickness of 1 μm or less was formed uniformly in the joint with a magnetic field as shown in Fig. 18 and the dashed line in Fig. 19. This

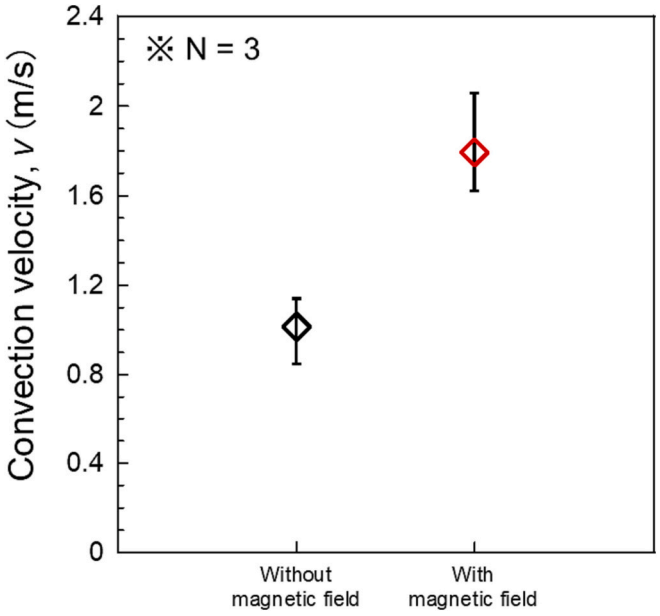

Fig. 24. Convection velocity for joints without and with magnetic field.

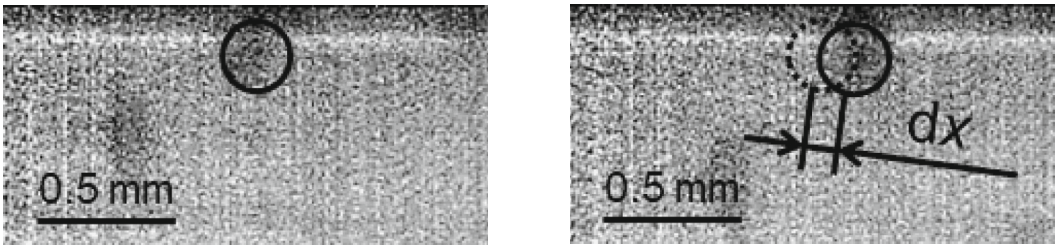

(a) t ms (b) $t + 0.1$ ms

Fig. 23. W particle movement distance during period of 0.1 ms. (a) t ms. (b) $t + 0.1$ ms.

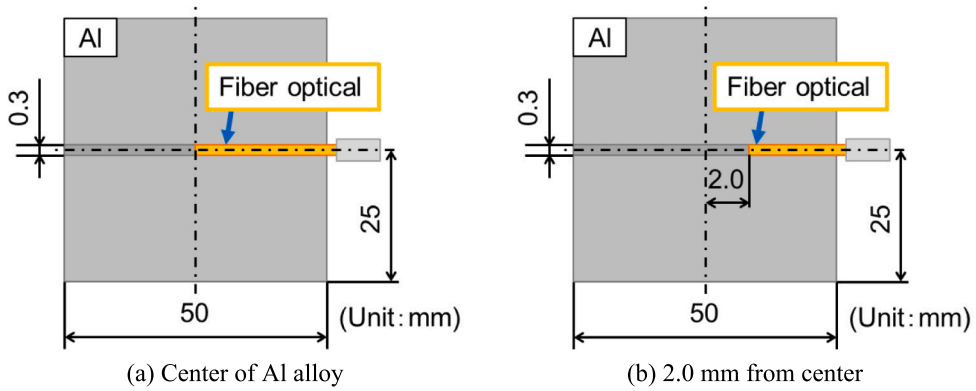

(a) Center of Al alloy (b) 2.0 mm from center

Fig. 25. Insertion position of fiber optic thermometer. (a) Center of Al alloy. (b) 2.0 mm from center.

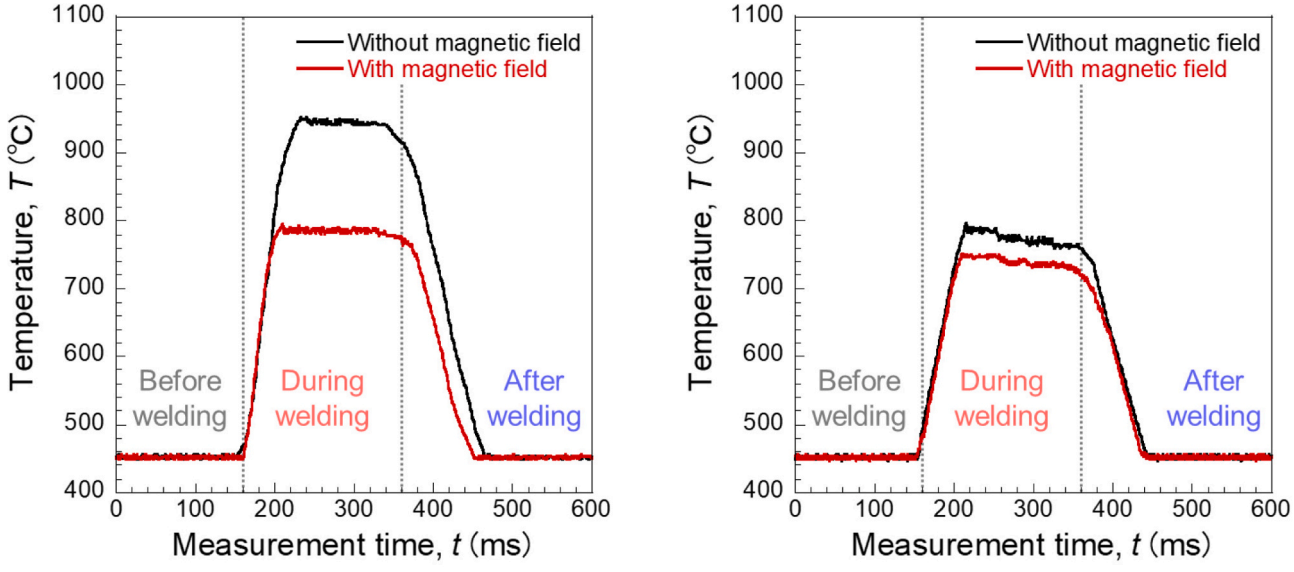

(a) Center of Al alloy (b) 2.0 mm from center

Fig. 26. Temperature history near center of joining interface. (a) Center of Al alloy. (b) 2.0 mm from center.

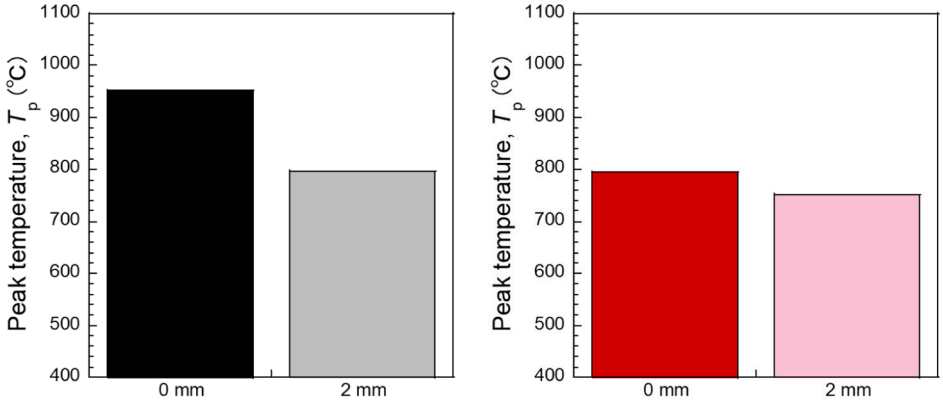

(a) Without magnetic field (b) With magnetic field

Fig. 27. Temperature difference near center of joining interface. (a) Without magnetic field. (b) With magnetic field.

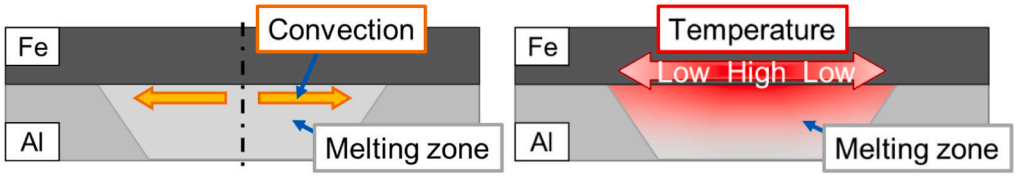

(a) Convection near joining interface (b) Temperature field near joining interface

Fig. 28. Convection and temperature field for joint without magnetic field. (a) Convection near joining interface. (b) Temperature field near joining interface.

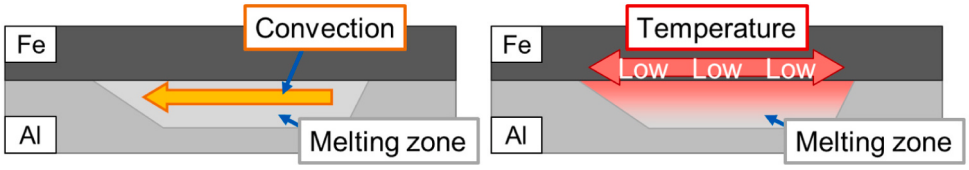

(a) Convection near joining interface (b) Temperature field near joining interface

Fig. 29. Convection and temperature field for joint with magnetic field. (a) Convection near joining interface. (b) Temperature field near joining interface.

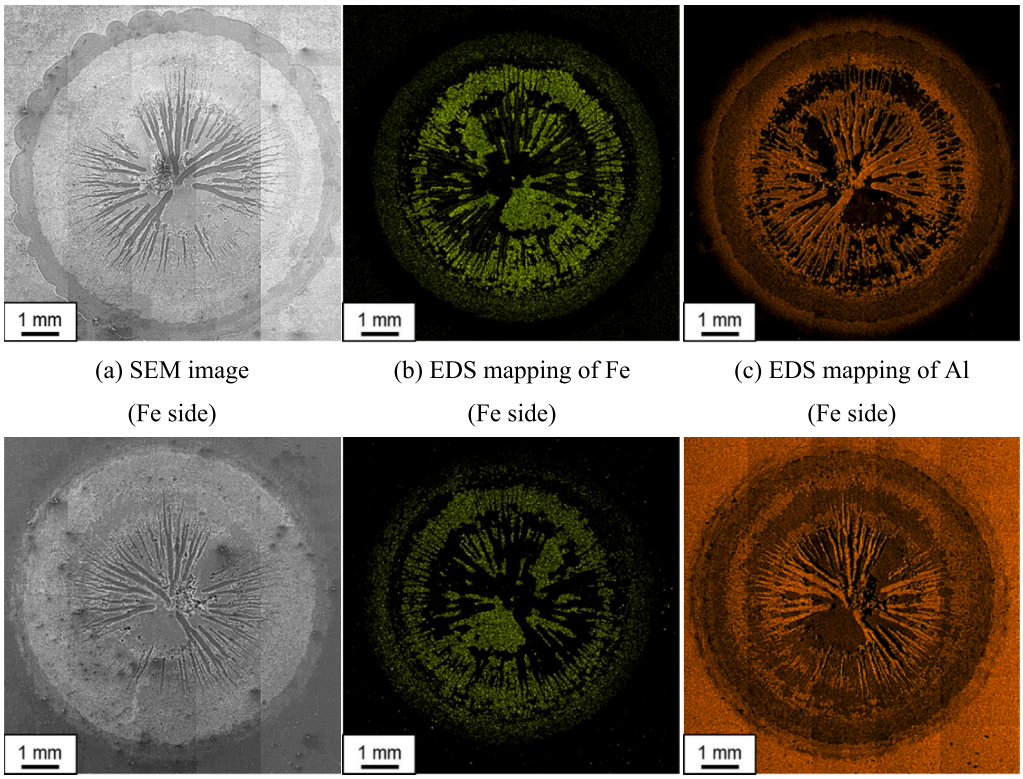

(a) SEM image (Fe side) (b) EDS mapping of Fe (Fe side) (c) EDS mapping of Al (Fe side)

(d) SEM image (Al alloy side) (e) EDS mapping of Fe (Al alloy side) (f) EDS mapping of Al (Al alloy side)

Fig. 30. Observation and analysis of fracture surface of joint without magnetic field. (a) SEM image (Fe side). (b) EDS mapping of Fe (Fe side). (c) EDS mapping of Al (Fe side). (d) SEM image (Al alloy side). (e) EDS mapping of Fe (Al alloy side). (f) EDS mapping of Al (Al alloy side).

suggests that the temperature field near the center of the joining interface was influenced by the change in convection under a magnetic field.

3.3. CTS of joint welded under magnetic field

Cross-sectional photographs of joints welded without and with a magnetic field after the cross tension test are shown in Fig. 20, and the CTS and load-displacement curve for each joint are shown in Figs. 21 and 22. Fig. 20 shows that both types of joint exhibited interface fracture. Moreover, Fig. 21 shows that the presence of a magnetic field increased the CTS for the joint. It is generally considered that during RSW of Fe and Al alloy, forming a thinner the IMC increases the strength of the joint [1–3]. Therefore, as shown in Figs. 18 and 19, it can be concluded that the CTS for the joint welded under a magnetic field is improved because a thin IMC is formed uniformly near the center of the joint. However, Fig. 22 shows that the displacement of the joint with a magnetic field increases as the load increases. This suggests that the joint failed ductilely compared to the joint without a magnetic field, but the

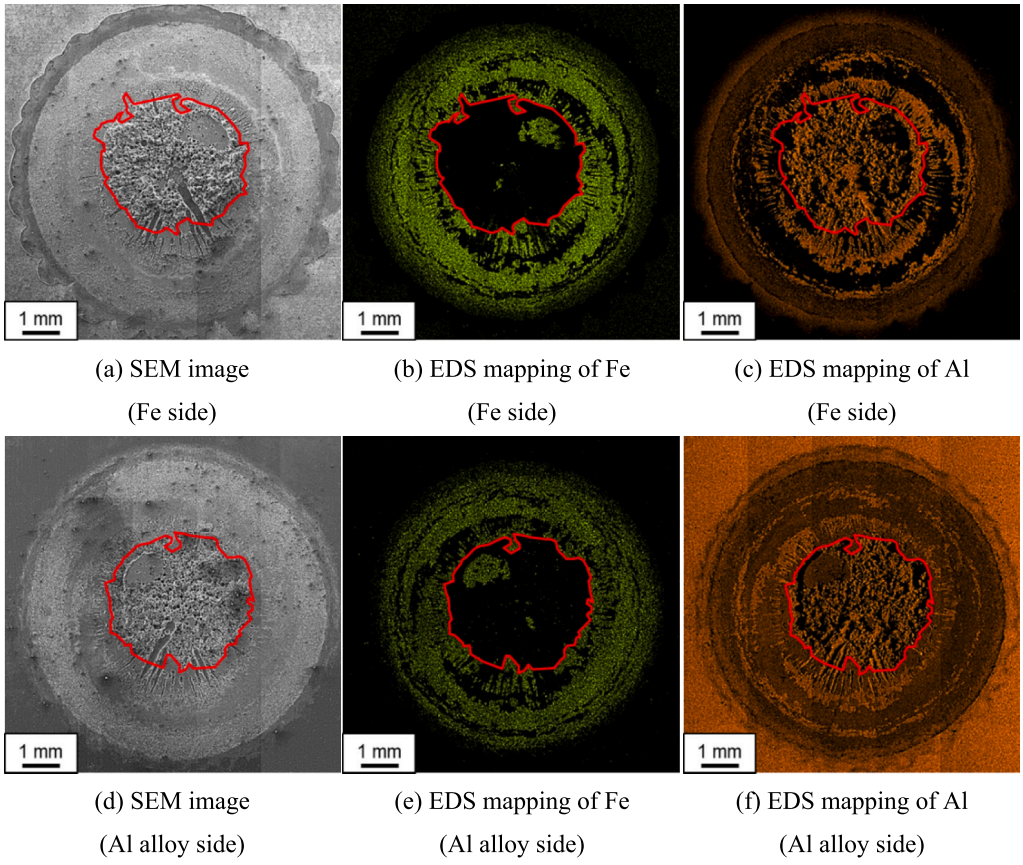

Fig. 31. Observation and analysis of fracture surface of joint with magnetic field. (a) SEM image (Fe side). (b) EDS mapping of Fe (Fe side). (c) EDS mapping of Al (Fe side). (d) SEM image (Al alloy side). (e) EDS mapping of Fe (Al alloy side). (f) EDS mapping of Al (Al alloy side).

joint failure mechanism during the cross tension test is not clear. In the next section, crack propagation during the cross tension test is examined, and the reason for the improved CTS for the joint welded under a magnetic field is discussed.

4. Discussion

4.1. Effect of magnetic field on driving force for convection

The results described in Section 3.2 suggest that the temperature field near the center of the joining interface changed in the joint welded in the presence of a magnetic field, but the effect of the change in convection is not clear. To clarify this, it is necessary to clarify the changes in heat transport near the center of the joining interface that accompany changes in convection. One factor that influences heat transport is the driving force for convection, which may be increased by the new electromagnetic force generated in the Al alloy melting zone by the application of a magnetic field. In this section, the convection velocity is used as an indicator of the convection driving force. The convection velocity in the Al alloy melting zone is calculated to determine the effect of a magnetic field. As shown in Fig. 23, from the X-ray transmission image obtained in the in-situ evaluation of convection (Section 3.1), the convection velocity was calculated by measuring the amount of W particle movement at the center during the late stage of energization, when the convection is stable.

The calculated convection velocity at the joint center is shown in Fig. 24, and it can be seen that it increases under a magnetic field. Furthermore, focusing on the maximum of the measured values, the convection velocity was approximately 1.14 m/s for the joint welded without a magnetic field. This is in relatively good agreement with the values determined from experimental and numerical simulations [19,20]. In contrast, in the presence of a magnetic field, the convection velocity was approximately 2.06 m/s. This suggests that the driving force for convection increases due to the generated electromagnetic force by the applying a magnetic field.

4.2. Effect of magnetic field on temperature field joining interface

To investigate the effect of the increased driving force for convection due to an applied magnetic field, the temperature near the center of the joining interface was measured. An immersion-type optical fiber thermometer manufactured by JFE Techno Research was used to measure the temperature. This thermometer consisted of three elements: a glass tube 0.25 mm in diameter, a stainless steel tube 1.4 mm in diameter protecting the glass tube, and a converter. The temperature measurement range of the thermometer was 500 to 1600 °C. The temperature measurement interval was set to 1.0 ms, and the temperature history was obtained from before power was applied until the lower limit of temperature measurement was reached after the power was applied. The temperature measurement points at the joining interface are shown in Fig. 25. From the IMC thickness distribution of each joint shown in Fig. 20, the diameter of the region of IMC formed depending on the temperature field at the joining interface is assumed to be about 4 mm, so an optical fiber was inserted so that its tip was at the center of the grooved Al alloy and 2.0 mm from the center of the Al alloy melting zone.

Fig. 26 shows the results for the positions shown in Fig. 25 for joints welded without and with a magnetic field. Fig. 26(a) shows that the temperature decreased significantly for the joint welded under a magnetic field compared to the joint without a magnetic field, the peak temperature from approximately 952.3 to 795.4 °C. Fig. 26(b) shows that the temperature 2.0 mm from the center of the joining interface also

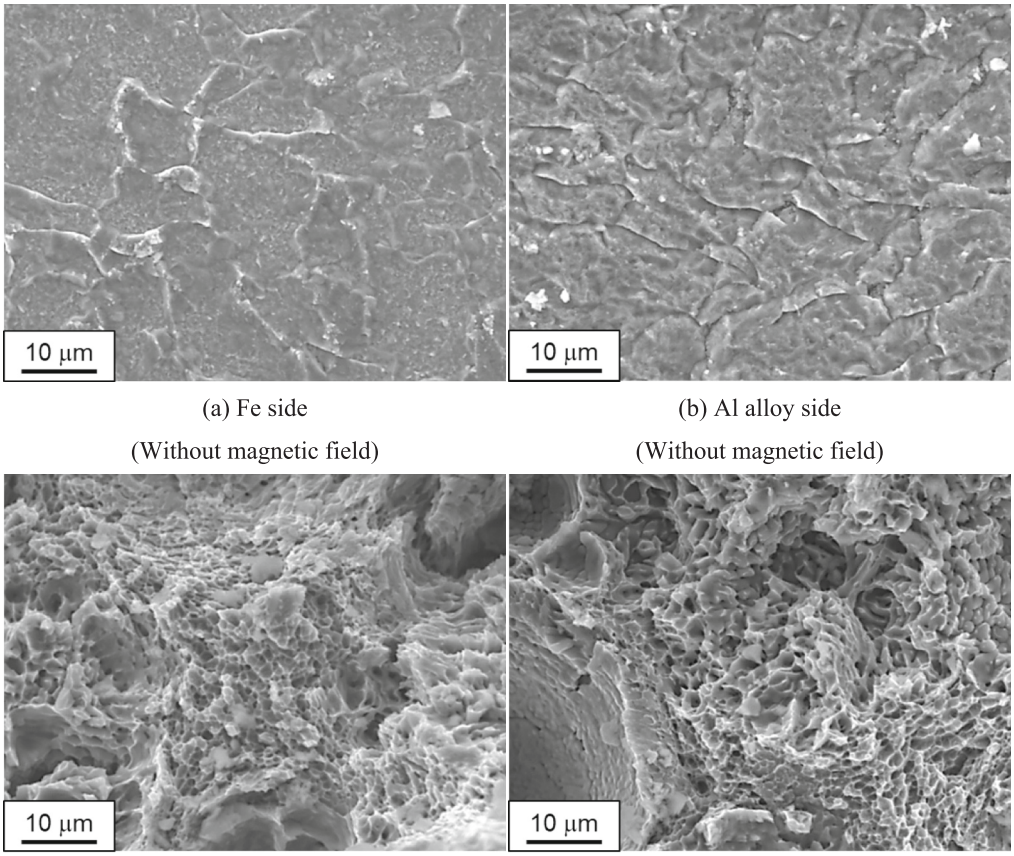

Fig. 32. SEM image magnifying center of fracture surface for joints without and with magnetic field. (a) Fe side (Without magnetic field). (b) Al alloy side (Without magnetic field). (c) Fe side (With magnetic field). (d) Al alloy side (With magnetic field).

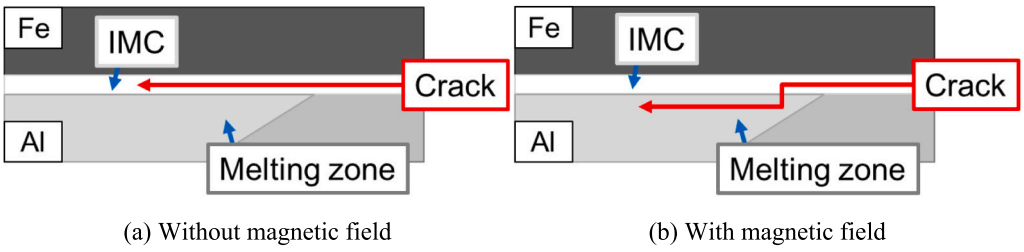

Fig. 33. Crack propagation behavior of joints subjected to cross tension tests. (a) Without magnetic field. (b) With magnetic field.

decreased for the case of a magnetic field, the peak temperature from approximately 795.8 to 752.2 °C. In addition, Fig. 27 shows the temperature difference of the peak temperature between the center of the joining interface and 2.0 mm from the center of the joining interface for each joint. It can be seen that the temperature difference of the peak temperature was smaller for the joint with a magnetic field than for the joint without a magnetic field.

The above results can be used to discuss changes in the temperature field associated with changes in convection behavior. Previous studies have reported that convection is driven axisymmetrically near the joining interface in a joint without a magnetic field, as shown in Fig. 28 (a) [19,20]. Therefore, it is considered that this convection causes heat transport from the center to the edge of the joining interface. Accordingly, it is inferred that a temperature gradient is generated near the center of the joining interface in the Al alloy melting zone in a joint without a magnetic field, as shown in Fig. 28(b). In contrast, as shown in Fig. 29(a), convection is considered to be driven in one direction near the joining interface in the joint welded in the presence of a magnetic field, based on the in-situ evaluation described in Section 3.1. In addition, the results discussed in the previous section suggest that the applying a magnetic field increases the driving force for convection. Therefore, enhanced heat transport in one direction along the joining interface is considered to occur. Accordingly, as shown in Fig. 29(b), the temperature near the center of the joining interface decreases and the temperature field becomes more uniform when a magnetic field is present during welding.

These results suggest that the temperature near the center of the joining interface is lowered and the temperature field is homogenized by the change in convection under a magnetic field, resulting in the formation of a thin and uniform IMC near the center. It was also found that changes in convection within the Al alloy melting zone have a significant effect on the state of IMC formation.

4.3. Crack propagation during cross tension tests

The IMC thickness distribution shown in Fig. 19 and the results of the cross tension tests shown in Fig. 21 suggest that the CTS for the joint welded under a magnetic field is improved because a thin IMC is formed uniformly near the center of the joint. Moreover, it has been reported that crack propagation during RSW of Fe and Al alloy changes during testing depending on the thickness of the IMC formed at the joining interface, which in turn changes the failure mechanism for the joint [3], but the failure mechanism for the joint subjected to the cross tension test in this experiment is not known. Therefore, to clarify the crack propagation behavior during the cross tension test, the fracture surfaces of the tested joint were observed to investigate the reason for the improved CTS for the joint welded under a magnetic field.

Figs. 30 and 31 show SEM images and EDS elemental maps for the fracture surfaces of joints welded without and with a magnetic field, respectively, following cross tension tests. As shown in Fig. 30, Fe and Al atoms were detected throughout the fracture surface on both the Fe and Al alloy sides of the joint without a magnetic field. In contrast, in Fig. 31, for the joint with a magnetic field, Fe and Al atoms were detected in the periphery of the fracture surface on both the Fe and Al alloy sides, but only Al atoms were detected near the center of the fracture surface, with almost no Fe atoms were detected in the area surrounded by the red line in the figure.

Fig. 32 shows magnified SEM images of the center of the fracture surface for the joint without a magnetic field, and the area surrounded by the red line in Fig. 31 for the joint with a magnetic field. The figure shows that both the Fe side and the Al alloy side of the joint without a magnetic field have quasi-cleavage fracture surfaces, while the joint with a magnetic field has dimple patterns on both the Fe side and the Al alloy side.

Based on these results, the crack propagation behavior and fracture mechanism of each joint is discussed. Because the IMC at the joining interface is formed by the interdiffusion of Fe and Al atoms, the IMC is thought to exist where Al atoms are detected on the fracture surface on the Fe side and where Fe atoms are detected on the fracture surface on the Al alloy side. Therefore, for the joint without a magnetic field, where Fe and Al atoms were detected over the entire fracture surface and quasi-cleavage fracture surfaces were observed, the crack propagates in the IMC, as shown in Fig. 33(a), and it is inferred that the joint fractured brittle. In contrast, for the joint with a magnetic field, Al atoms were detected near the center of the fracture surface, but no Fe atoms were detected, suggesting that IMC is not present in this area. In addition, dimple patterns were observed in the area where no Fe atoms were detected, suggesting that the crack propagated in the IMC near the edge and then in the Al alloy melting zone near the center in the joint with a magnetic field, as shown in Fig. 33(b), and it is inferred that the joint fractured ductilely.

These results suggest that in the joint with a magnetic field, the IMC is formed thin and uniform near the center, so that the crack is difficult to propagate in the IMC, and as a result, the crack near the center propagates from the IMC into the Al alloy melting zone and the joint ductile fracture, thereby improving the CTS.

5. Conclusions

In this study, convection in the Al alloy melting zone during RSW of Fe and Al alloy was varied by applying a magnetic field and its effect on joint characteristics was investigated. The results showed the following:

- In-situ evaluation of convection using synchrotron radiation revealed that an applied magnetic field caused a non-axisymmetric change in convection in the Al alloy melting zone.
- The change in convection caused by the magnetic field deflected the Al alloy melting zone and formed a thin uniform IMC near the center.
- The convection velocity in the Al alloy melting zone increased in the joint welded under a magnetic field, suggesting that the driving force for convection was increased.
- The increase in the driving force enhanced heat transport by convection near the joining interface, resulting in a decrease in temperature and homogenization of the temperature field, suggesting that the IMC formed near the center was thin and uniform.
- Cross tension tests confirmed that the CTS for the joint welded under a magnetic field improved due to the formation of a thin uniform IMC near the center.
- The results of fracture surface observation and elemental analysis of the joint subjected to cross tension testing indicated that the crack propagated from the inside of the IMC to the Al alloy melting zone in the joint welded under a magnetic field, suggesting that the CTS was improved by ductile fracture of the joint as a result of the crack.

These results suggest that the external magnetic field has a significant effect on the joint characteristics of Fe-Al dissimilar material RSW. However, a quantitative evaluation of the external magnetic field has not yet been performed, and analytical experiments, such as investigations of the most suitable magnet placement and magnetic field strength, are needed. In addition, the observation method of convection in-situ evaluation using synchrotron radiation, the image processing method of X-ray transmission image, and the analysis method should be further improved in the future.

Declaration of competing interest

The authors declare that they have no known competing financial interests or personal relationships that could have appeared to influence the work reported in this paper.

Acknowledgements

This paper is based on results obtained from a project, JPNP14014, commissioned by the Japan New Energy and Industrial Technology Development Organization. Some synchrotron radiation experiments were performed at the BL14B1 of SPring-8 with the approval of the Japan Synchrotron Radiation Research Institute (Proposal Nos. 2020A3689 and 2019B3689). The authors would like to thank Dr. Shiro of the National Institutes for Quantum Science and Technology, Japan, for her significant help with the fundamental experiments at BL14B1 and technical support for this experiment. Also, we would like to thank Mr. Nagase, Mr. Tachibana, Mr. Koizumi, Mr. Ogishi, and Mr. Kondo, students of the Osaka Institute of Technology, for conducting many experiments related to this research.

Appendix A. Supplementary data

Supplementary data to this article can be found online at https://doi.org/10.1016/j.jmapro.2024.01.049.

References

[1] Miyamoto K, Nakagawa S, Sugi C, Sakurai H, Hirose A. Dissimilar joining of aluminum alloy and steel by resistance spot welding. SAE Int J Mater Manuf 2009; 2(1):58–67. https://doi.org/10.4271/2009-01-0034.
[2] Kumamoto K, Shohji I, Kobayashi T, Iyota M. Effect of microstructure on joint strength of Fe/Al resistance spot welding for multi-material components. Mater Sci Forum 2021;1016:774–9. https://doi.org/10.4028/www.scientific.net/MSF.1016.774.
[3] Chen N, Wang HP, Carlson BE, Sigler DR, Wang M. Fracture mechanisms of Al/steel resistance spot welds in coach peel and cross tension testing. J Mater Process Technol 2018;252:348–61. https://doi.org/10.1016/j.jmatprotec.2017.09.035.
[4] Chen N, Wan M, Wang HP, Wan Z, Carlson BE. Microstructure and mechanical evolution of Al/steel interface with Fe_2Al_5 growth in resistance spot welding of aluminum to steel. J Manuf Process 2018;34(A):424–34. https://doi.org/10.1016/j.jmapro.2018.06.024.

[5] Rao HM, Kang J, Shi L, Sigler DR, Carlson BE. Effect of specimen configuration on fatigue properties of dissimilar aluminum to steel resistance spot welds. Int J Fatigue 2018;116:13–21. https://doi.org/10.1016/j.ijfatigue.2018.06.009.
[6] Zhang W, Sun D, Han L, Li Y. Optimized design of electrode morphology for novel dissimilar resistance spot welding of aluminium alloy and galvanized high strength steel. Mater Des 2015;85:461–70. https://doi.org/10.1016/j.matdes.2015.07.025.
[7] Lara B, Giorjao R, Ramirez A. Resistance spot welding of printed interlayers to join Al-Fe sheets. Science and Technology of Welding and Joining 2023;28(1):18–26. https://doi.org/10.1080/13621718.2022.2108999.
[8] Das T, Das R, Paul J. Resistance spot welding of dissimilar AISI-1008 steel / Al-1100 alloy lap joints with a graphene interlayer. J Manuf Process 2020;53:260–74. https://doi.org/10.1016/j.jmapro.2020.02.032.
[9] Hu S, Haselhuhn AS, Ma Y, Li Z, Qi L, Li Y, et al. Effect of external magnetic field on resistance spot welding of aluminium to steel. Science and Technology of Welding and Joining 2022;27(2):84–91. https://doi.org/10.1080/13621718.2021.2013707.
[10] Iyota M, Hamaguchi T, Koga Y. Dissimilar joining of high-strength steel and aluminum alloy using resistance spot welding with die- and punch-shaped electrodes. Eng Proc 2023;43(1):45. https://doi.org/10.3390/engproc2023043045.
[11] Li P, Chen S, Dong H, Ji H, Li Y, Guo X, et al. Interfacial microstructure and mechanical properties of dissimilar aluminum/steel joint fabricated via refilled friction stir spot welding. J Manuf Process 2020;49:385–96. https://doi.org/10.1016/j.jmapro.2019.09.047.
[12] Feizollahi V, Moghadam AH. Effect of pin geometry, rotational speed, and dwell time of tool in dissimilar joints of low-carbon galvanized steel and aluminum 6061-T6 by friction stir spot welding. Results Mater 2023;20:100483. https://doi.org/10.1016/j.rinma.2023.100483.
[13] Cui L, Wei Z, Ma B, He D, Huang H, Cao Q. Microstructure inhomogeneity of dissimilar steel/Al butt joints produced by laser offset welding. J Manuf Process 2020;50:561–72. https://doi.org/10.1016/j.jmapro.2020.01.011.
[14] Chen X, Wang X, Liu Z, Hu Z, Huan P, Yan Q, et al. Effect of Cu content on microstructure transformation and mechanical properties of Fe-Al dissimilar laser welded joints. Opt Laser Technol 2020;126:106078. https://doi.org/10.1016/j.optlastec.2020.106078.
[15] Abe Y, Fujimoto T, Nakatani M, Komen H, Shigeta M, Tanaka M. High speed X-ray observation of digital controlled submerged arc welding phenomena. Science and Technology of Welding and Joining 2021;26(4):332–40. https://doi.org/10.1080/13621718.2021.1908746.
[16] Komen H, Shigeta M, Tanaka M, Abe Y, Fujimoto T, Nakatani M, et al. Numerical investigation of heat transfer during submerged arc welding phenomena by coupled DEM-ISPH simulation. Int J Heat Mass Transf 2021;171:121062. https://doi.org/10.1016/j.ijheatmasstransfer.2021.121062.
[17] Miyagi M, Wang H, Yoshida R, Kawahito Y, Kawakami H, Shobu T. Effect of alloy element on weld pool dynamics in laser welding of aluminum alloys. Sci Rep 2018;8:12944. https://doi.org/10.1038/s41598-018-31350-4.
[18] Li YB, Lin ZQ, Qi Shen, Lai XM. Numerical analysis of transport phenomena in resistance spot welding process. J Manuf Sci Eng 2011;133(3):031019. https://doi.org/10.1115/1.4004319.
[19] Iyota M, Matsuda T, Sano T, Shigeta M, Shobu T, Yumoto H, et al. A study on convection in molten zone of aluminum alloy during Fe/Al resistance spot welding. J Manuf Process 2023;94:424–34. https://doi.org/10.1016/j.jmapro.2023.03.032.
[20] Chikuchi S, Shigeta M, Komen H, Tanaka M. Particle simulation of nugget formation process during steel/aluminum alloy dissimilar resistance spot welding and thickness estimation of intermetallic compounds. Weld Int 2022;36(7):434–42. https://doi.org/10.1080/09507116.2022.2084821.
[21] Miyamoto K, Nakagawa S, Tsushima K, Katayama T, Iwatani S, Hojo S, et al. Effect of Zn insertion on diffusion bonded joint properties of steel and aluminum alloy - dissimilar metals joining of steel and aluminum alloy by Zn insertion. Q J Jpn Weld Soc 2014;32(1):15–30. https://doi.org/10.2207/qjjws.32.15 [in Japanese].